energy&fuels

Article

pubs.acs.org/EF

# Laminar Flame Characteristics of *iso*-Octane/*n*-Butanol Blend−Air Mixtures at Elevated Temperatures

Xinyi Zhang, Chenglong Tang,* Huibin Yu, Qianqian Li, Jing Gong, and Zuohua Huang*

State Key Laboratory of Multiphase Flow in Power Engineering, Xi'an Jiaotong University, Xi'an 710049, China

Supporting Information

**ABSTRACT:** In this work, laminar flame speeds and Markstein lengths of *iso*-octane/*n*-butanol−air mixtures were measured via the outwardly expanding spherical flame method and high-speed schlieren photography over a wide range of equivalence ratios and blending ratios of *n*-butanol at elevated initial temperatures. Results show that laminar flame speeds of fuel blends slightly increase with increasing blending ratio of *n*-butanol. The effect of blending ratio on laminar flame speed of fuel blends was mechanistically interpreted through examining the thermodynamic and diffusive property, as well as the overall oxidation kinetics. Measurements on the burned gas Markstein length show a generalized behavior. There exists a minimum absolute Markstein length at the critical equivalence ratio $\phi^*$, under which the stretch effect on the flame propagating speed is minimized. At equivalence ratios less than $\phi^*$, Markstein length is decreased with increasing blending ratio of *n*-butanol, indicating that the addition of *n*-butanol reduces the diffusional thermal stability of the blend; while at equivalence ratios larger than $\phi^*$, Markstein length increases with increasing blending ratio of *n*-butanol. This experimental observation on the Markstein length is consistent with the theoretical investigation. A correlation of laminar flame speed of *n*-butanol/iso-octane blend as a function of equivalence ratio, temperature, and blending ratio of *n*-butanol is given on the basis of experimental data.

## 1. INTRODUCTION

Biofuels, being renewable and ecofriendly, have been considered as promising alternative fuels for engines. In 2012, the International Energy Agency (IEA) laid out a "road map" to ramp up the use of biofuels from around 2% of global transportation fuel today up to 27% by the year 2050.[1] Recently, as one representative biofuel, *n*-butanol has attracted much attention in the engine and combustion community, owing to its high energy density and good solubility in both gasoline and diesel. Compared to ethanol and methanol, *n*-butanol is much less hydrophilic and much less corrosive to existing fuel pipelines,[1] easier to mix with gasoline thanks to its longer alkyl carbon chain, and safer in storage and transportation because of its lower vapor pressure, and it also performs better in cold start of engines because of its lower enthalpy of vaporization.[2,3] Furthermore, *n*-butanol has higher energy density, which helps to improve fuel economy. The physical properties of pure gasoline and alcohols are listed in Table 1. However, the potential of *n*-butanol is limited by its production.[1] Since the traditional raw material for *n*-butanol production is cereal crops, sugar cane, and cellulosic plants, among which cereal crops and sugar cane are food, a food-versus-fuel conundrum will appear if *n*-butanol is produced in large scale, and the cost of production will become high. Scientists are now working hard on innovative technology to realize massive production of *n*-butanol through a variety of methods,[1] However, at present, pure *n*-butanol as engine fuel is still expensive. Thus, the utilization of *n*-butanol/gasoline fuel blends is regarded as the practical and cost-effective choice for engines in the current stage.

Previous studies on *n*-butanol/gasoline blends mainly concentrated on engine combustion and emissions. Alasfour[4] studied the engine thermal efficiency of a single-cylinder engine fueled with a 30% *n*-butanol/70% gasoline blend, and 7% reduction in power output was found compared to engines fueled with pure gasoline. Gu et al.[5] found that blending *n*-butanol decreases the specific HC, CO, and $NO_x$ emissions and particle number concentration compared to pure gasoline. Szwaja and Naber[6] observed that combustion duration and rate of MFB (mass fraction burned) of *n*-butanol blended gasoline are comparable to those of pure gasoline at blending ratios of 20% and 60%, and their study indicated that *n*-butanol could fully or partially substitute gasoline from the combustion and energy density perspective. Compared to the engine studies,

**Table 1. Physical Properties of Pure Gasoline and Alcohols[38−40]**

| | methanol | ethanol | *n*-butanol | gasoline |
|---|---|---|---|---|
| chemical formula | $CH_3OH$ | $C_2H_5OH$ | $C_4H_9OH$ | $C_4$−$C_{12}$ |
| density (kg/m$^3$) | 791.3 | 789.4 | 809.7 | 715−765 |
| oxygen content (mass %) | 0.5 | 0.35 | 0.22 | 0 |
| energy-volume density (kJ/cm$^3$) | 15.78 | 21.11 | 26.90 | 31.87 |
| cctane number, $(R + M)/2$ | 100 | 100 | 87 | 90 |
| lower heating value (MJ/kg) | 19.6 | 26.8 | 33.1 | 42.7 |
| enthalpy of vaporization (kJ/g) | 1098.63 | 837.86 | 584.19 | 348.88 |
| solubility in water at 20 °C (mL/100 mL of $H_2O$) | fully miscible | fully miscible | 7.7 | <0.1 |

**Received:** January 29, 2013
**Revised:** March 19, 2013
**Published:** March 19, 2013

ACS Publications © 2013 American Chemical Society

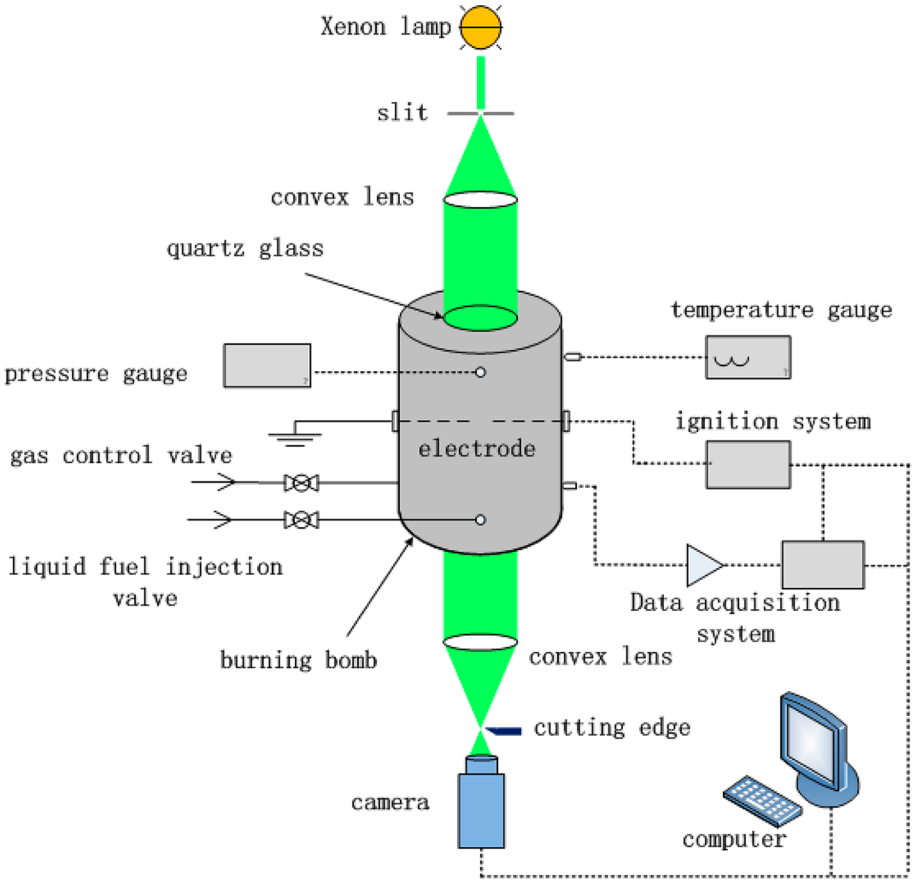


**Figure 1.** Experimental apparatus.

fundamental studies of *n*-butanol/gasoline blends are still limited. Dagaut and co-workers[7−10] performed a series of experiments on the oxidation kinetics of alcohol (methanol, ethanol, and *n*-butanol)/gasoline blends in a fused silica jet-stirred reactor in recent years and gave the concentration profiles of reactants, stable intermediates, and final products under different conditions and blending ratios of alcohol. On the basis of their experimental results, chemical mechanisms of alcohol/gasoline blends were proposed, and results showed that increasing the initial fraction of alcohol in the fuel blend would increase the importance of its production routines for the formation of products they measured.

Laminar flame speed is a key parameter of fuel as it embodies the physicochemical properties of combustible mixtures such as reactivity, diffusivity, and exothermicity. Laminar flame speed has a significant effect on the performance and pollutant emissions of internal combustion engines. Additionally, laminar flame speed is the basic parameter in turbulent flame modeling and engine combustion simulations.[11] Furthermore, laminar flame speed has been constantly used to validate the chemical kinetic mechanism. Although laminar flame speeds of pure fuels have been extensively investigated, studies on blended fuels are still limited, especially for the liquid blended fuels.[12,13] Gulder[14] determined the laminar flame speeds of methanol/*iso*-octane blends. This study showed that although pure methanol burns faster than pure *iso*-octane, the laminar flame speed of methanol/*iso*-octane blends decreases with the addition of methanol.[14] Gulder[14] attributed this to the assumption that methanol suppresses the overall reactivity of mixtures by providing the species of $CH_2O$ and removing the intermediate radicals through $R + CH_2O \rightarrow CHO + RH$. The laminar flame speed of *n*-butanol/*iso*-octane blends was first given by Broustail et al.[15] using a closed combustion chamber. Subsequently, they extended their experimental conditions to elevated pressures.[16] Their work showed that the laminar flame speed of *n*-butanol/*iso*-octane blends increases monotonically with increasd blending ratio of *n*-butanol (volume fraction of *n*-butanol in the binary fuel blend, $f_{vb}$) at different initial pressures up to 1.0 MPa. At elevated pressures, the difference in laminar flame speeds between *n*-butanol and *iso*-octane decreases. However, laminar flame speeds and instability at varied initial temperatures were not characterized. As temperature is an important parameter that affects the flame propagation in a practical combustion facility, experimental data at elevated temperatures are needed for development and validation of the chemical kinetic mechanism of *iso*-octane/*n*-butanol blends. Additionally, the effects of *n*-butanol addition on laminar flame speed and Markstein length of the fuel blends have not been analyzed theoretically. In this study, first, we measured the laminar flame speeds of *n*-butanol/*iso*-octane blend−air mixtures over a wide range of equivalence ratios and *n*-butanol blending ratios at elevated temperatures. Second, we clarified the relationship between laminar flame speed and blending ratio of *n*-butanol, adiabatic temperature, overall diffusive nature, and oxidation kinetics of the fuel blend/air mixtures. The dependence of Markstein length on blending ratio of *n*-butanol was also interpreted. Finally, we correlated the laminar flame speed against the temperature, blending ratio of *n*-butanol, and equivalence ratio.

## 2. EXPERIMENTAL SECTION

The experimental apparatus has been described in details in previous literature.[17,18] Here, only a brief description is given. Basically, the whole system consists of a combustion chamber with a heating system, a mixture preparation system, an ignition system, a data acquisition system, and a high-speed schlieren photography system, as shown in Figure 1.

In experiments, the chamber was first heated to the desired initial temperature by a heating tap. The combustion chamber is cylindrical with diameter of 180 mm and length of 210 mm, and the initial temperature is measured by a thermocouple with an uncertainty of ±3 K. The preblended liquid fuel blends were then injected into the chamber via microsyringes. Purities of *n*-butanol and *iso*-octane in the study are 99.5% and 99%, respectively. Nitrogen and oxygen were introduced into the chamber through the intake port with a molar ratio of 3.762, similar to the air. At least 5 min elapsed before ignition, to ensure fuel vaporization and complete mixing. A wait period of half an hour was tested and no appreciable difference was observed. To capture the whole flame propagation process, the Redlake HG-100K high-speed camera operating at 10 000 frames/s was set to trigger 0.3 s earlier than the ignition timing. Each time after combustion, the exhaust gas in chamber was vacuumed and the chamber was flushed with fresh air at least three times before the next run, so as to eliminate the effect of residual gas in the chamber.

For the spherically expanding flame, the stretched flame speed (flame propagation speed) is directly obtained from the raw flame radius ($r_f$)−time ($t$) history through

$$S_b = dr_f/dt \tag{1}$$

The stretch rate, which is induced by local flow straining, flame curvature, and flame unsteadiness,[19] is then derived through

$$\alpha = \frac{1}{A}\frac{dA}{dt} = \frac{2}{r_f}\frac{dr_f}{dt} = \frac{2}{r_f}S_b \tag{2}$$

For weakly stretched flame, the flame propagation speed and stretch rate are linearly correlated as

$$S_b^0 = S_b - L_b\alpha \tag{3}$$

where $S_b^0$ is the laminar flame speed with respect to the burned gas and $L_b$ is the burned gas Markstein length. On the basis of mass conservation across the flame front, the laminar flame speed of the unburned gas, $S_u^0$, is calculated as

$$S_u^0 = \rho_b S_b^0/\rho_u \tag{4}$$

In this study, fuel blends with six blending ratios ($f_{vb}$ = 0, 0.2, 0.4, 0.6, 0.8, and 1.0) were tested. Initial temperatures are 353, 393, and 433 K with an uncertainty of 3 K, and equivalence ratios vary from 0.8 to 1.5 with an interval of 0.1. All the experiments were carried out at 0.1 MPa, and each case was repeated at least three times to verify the repeatability of experiment.

## 3. RESULTS AND DISCUSSION

**3.1. System Validation.** Figure 2 illustrates the measured laminar flame speeds of (a) *iso*-octane−air and (b) *n*-butanol−air mixtures, along with the previous data. For *iso*-octane−air mixtures, the measurements of Kelley et al.[20] were conducted using both the counterflow flame and spherically expanding flame, and perfect agreement was found between the two sets of measurements. The measurements in this study agree fairly well with the data in the literature[19] over a wide range of equivalence ratios. Additionally, the measurements of Broustail et al.[16] present slightly lower values due to its lower initial temperature. For *n*-butanol−air mixtures, the measurements in this study show good agreement with those of Liu et al.[21] over a wide range of equivalence ratios. Compared to the measurements of Gu et al.[22] and Broustail et al.,[16] the present data give slightly higher values due to a higher initial temperature. Figure 3 exhibits the burned gas Markstein lengths of (a) *iso*-octane−air and (b) *n*-butanol−air mixtures. It is found that the burned gas Markstein length decreases with increasing equivalence ratio, which is consistent with the results of Broustail et al.[15,16] and Bradley et al.[23]

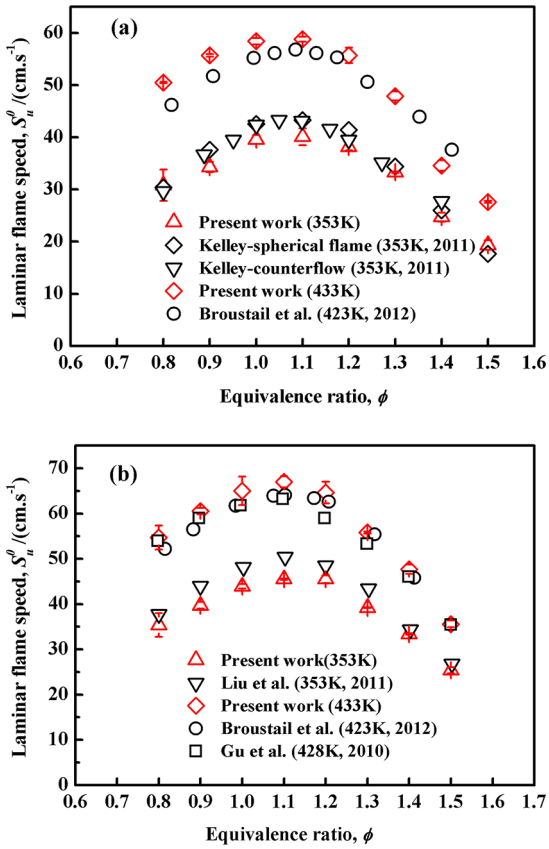


**Figure 2.** Laminar flame speed of fuel−air mixtures versus equivalence ratio at initial pressure of 0.1 MPa. (a) *iso*-Octane−air mixtures; (b) *n*-butanol−air mixtures.

**3.2. Laminar Flame Speeds.** *3.2.1. Raw Laminar Flame Speed Data.* Figure 4 gives the laminar flame speed of the binary fuel blend−air mixtures at three initial temperatures as a function of blending ratios of *n*-butanol, $f_{vb}$. Under all conditions, laminar flame speed shows a small increase with increasing blending ratio of *n*-butanol. The increase of laminar flame speed is even more inconspicuous when the mixture is close to the stoichiometry. Figure 5 shows the dependence of laminar flame speed on equivalence ratio for *iso*-octane/*n*-butanol−air mixtures at different blending ratios and initial temperatures. It is noted that the peak value of laminar flame speed moves to the fuel-richer side with increasing blending ratio of *n*-butanol. Oxygenated fuels were reported to have higher reactivities in the fuel-rich region compared to pure *n*-alkanes.[24−26]

*3.2.2. Interpretation of the Effect of Blending Ratio of n-Butanol on Laminar Flame Speed.* It is noted that the laminar flame speeds of the binary fuel−air mixtures at all equivalence ratios and temperatures show a slightly positive dependence on the blending ratio of *n*-butanol. The mechanism of this behavior is analyzed below. Laminar burning flux, $f = \rho_u S_u^0$, can be simply evaluated as[27]

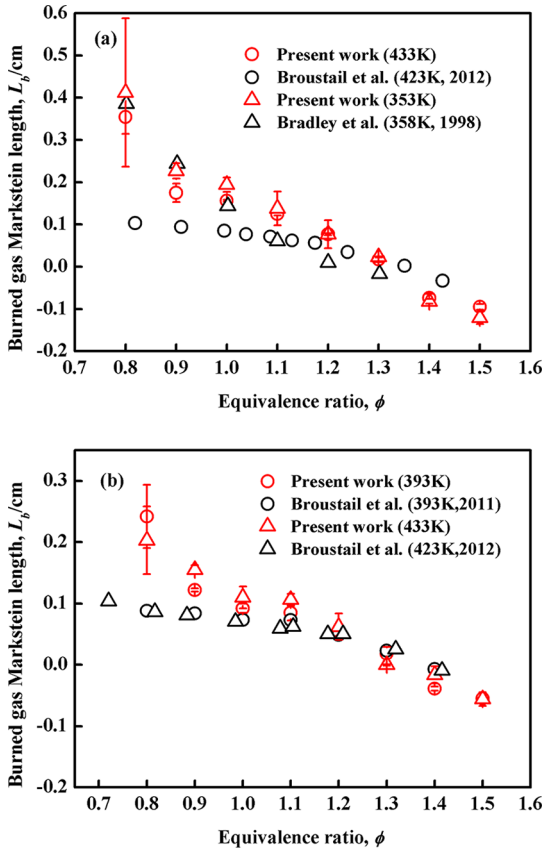


**Figure 3.** Burned gas Markstein length of fuel−air mixtures versus equivalence ratio at initial pressure of 0.1 MPa. (a) *iso*-Octane−air mixtures; (b) *n*-butanol−air mixtures.

$$f^2 \propto (\lambda/C_p)Le[\exp(-E_a/R_0T_{ad})] \quad (5)$$

where $\lambda/C_p$ is the density-compensated thermal diffusivity, $Le$ is the global Lewis number, $E_a$ is the overall activation energy, and $T_{ad}$ is the adiabatic temperature. $(\lambda/C_p)Le$, $T_{ad}$, and $E_a$ represent transport property, thermodynamic property, and oxidation kinetics, respectively. As the gas density of *n*-butanol−air mixtures is a little higher than that of *iso*-octane−air mixtures, the governing physics that determines the trend in Figure 4 can also be analyzed from these three factors.

For the unburned mixtures containing fuels of similar structure, the difference in laminar flame speed directly correlates to the difference in adiabatic temperature,[25] but it may be different for those that contain fuels of different structure. As shown in Figure 6, the adiabatic temperature of the binary fuel−air mixtures is slightly decreased with increasing blending ratio of *n*-butanol. This is reasonable since the energy density of *n*-butanol is 10% lower than that of *iso*-octane, which results in a decreased adiabatic temperature of *n*-butanol. Thus, it is concluded that thermal property is not the factor that increases the laminar flame speed when *n*-butanol is added.

The Lewis number, $Le$, is calculated by the method proposed by Lowry et al.:[28]

$$Le = \lambda/\rho C_p D_m \quad (6)$$

where $\lambda/\rho C_p$ represents mass diffusivity of the binary fuel−air mixtures and $D_m$ is mass diffusivity of the deficient reactant to the abundant inert, which is $N_2$ in this study. The Lennard-Jones potential data of the fuel blends are the mass average of parameters of the pure fuels. As shown in Figure 7, Lewis number decreased with increasing blending ratio of *n*-butanol under both lean and rich mixture conditions. Figure 8 illustrates the density-compensated thermal diffusivity of the mixtures as a function of the blending ratio of *n*-butanol. Thermal diffusivity is also decreased with increasing blending ratio of *n*-butanol. Thus, the thermal diffusivity weighted Lewis number $(\lambda/C_p)Le$ in eq 5 decreased with increasing blending ratio of *n*-butanol.

As both $T_{ad}$ and $(\lambda/C_p)Le$ exert a negative influence on laminar flame speed of the binary fuel with increasing blending ratio of *n*-butanol, it is speculated that oxidation kinetics is the factor that makes a positive correlation between laminar flame

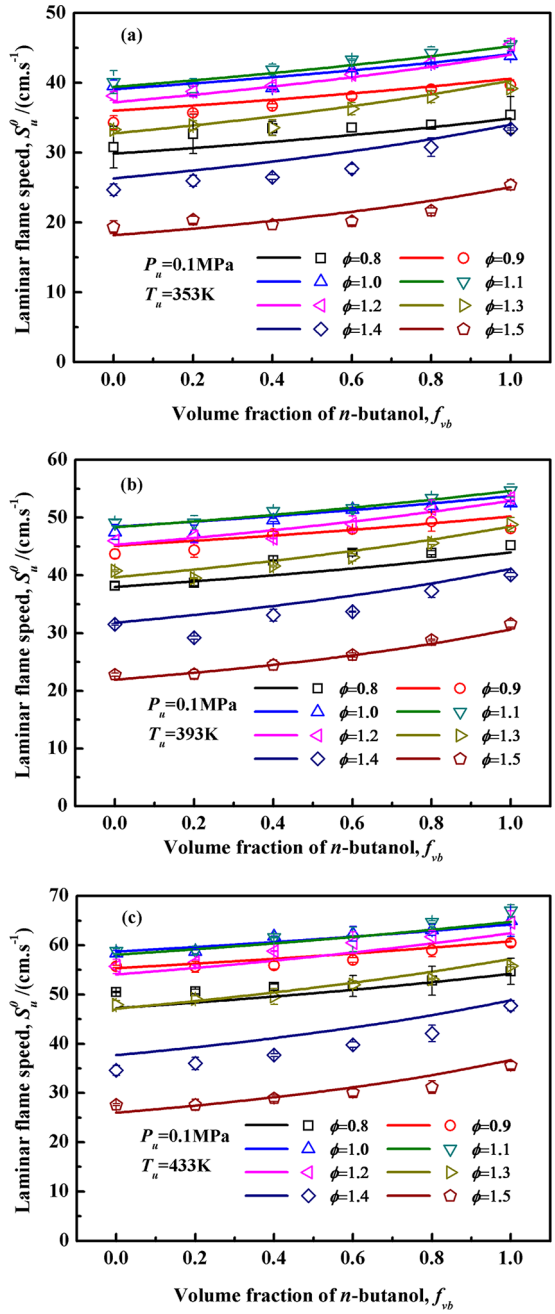


**Figure 4.** Laminar flame speed versus volume fraction of *n*-butanol at different equivalence ratios. (a) $T_u$ = 353 K; (b) $T_u$ = 393 K; (c) $T_u$ = 433 K. Symbols, experimental data; lines, eq 11 discussed in section 3.4.

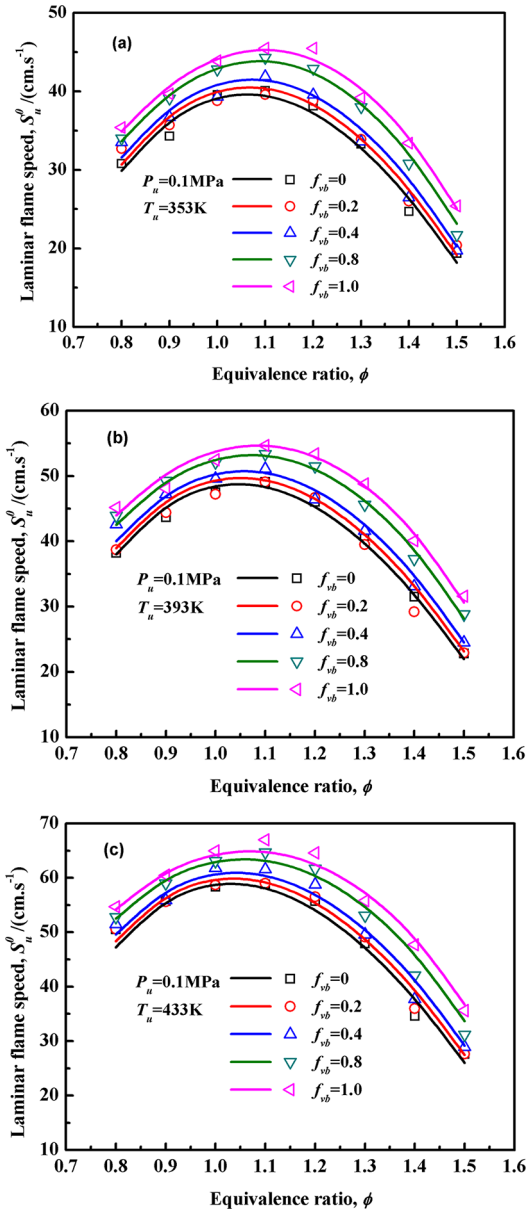


**Figure 5.** Laminar flame speed versus equivalence ratio at different blending ratios. (a) $T_u$ = 353 K; (b) $T_u$ = 393 K; (c) $T_u$ = 433 K. Symbols, experimental data; lines, eq 11 discussed in section 3.4.

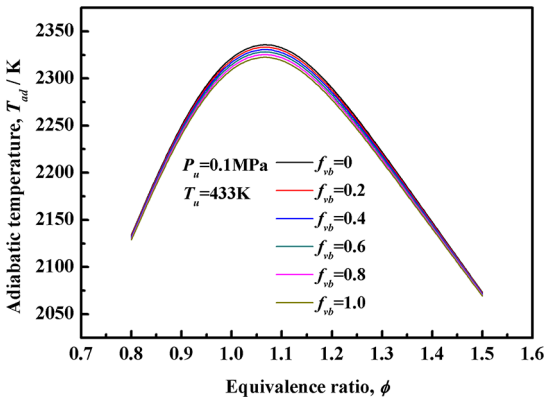


**Figure 6.** Adiabatic temperature versus equivalence ratio at different blending ratios.

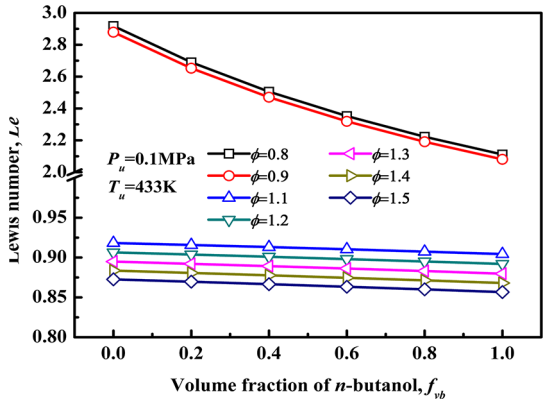


**Figure 7.** Lewis number of *iso*-octane/*n*-butanol blend−air mixtures.

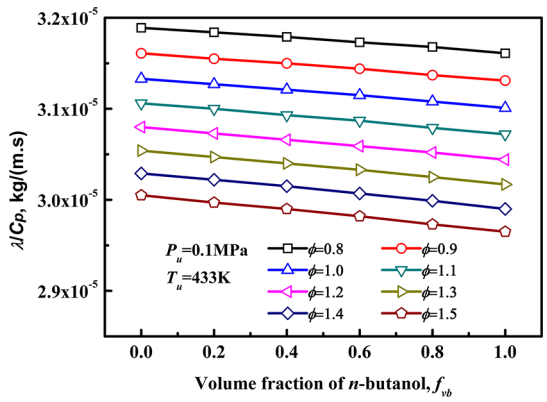


**Figure 8.** Density-compensated thermal diffusivity of *iso*-octane/*n*-butanol blend−air mixtures.

speed and blending ratio of *n*-butanol. Davis and Law[25] compared the flame speed of *n*-butane with that of *iso*-octane. They found that the flame speed of *iso*-octane is lower than that of *n*-butane. Due to the very close adiabatic temperature and thermal diffusivity of the two fuels, they stated that the branched-chain structure accounts for the reduction of flame speed of *iso*-octane through oxidation kinetics compared to that of *n*-butane. Ji et al.[29] confirmed Davis and Law's result and pointed out that the branched-chain structure decreases the flame speed of *iso*-octane by producing notably high amounts of methyl ($CH_3$), propene ($C_3H_6$), and *iso*-butene ($iC_4H_9$) radicals, which scavenge the H radicals and reduce the overall reactivity. Veloo et al.[26] experimentally investigated the laminar flame speeds of both *n*-butanol and *n*-butane, and very close values were obtained over the entire range of equivalence ratios because the two fuels give balanced production of $CH_3$ and H radicals during the oxidation process. On the basis of previous studies, it can be concluded that although *n*-butane and *n*-butanol give balanced production of $CH_3$ and H, the high amounts of unreactive and H-scavenging intermediates decrease the laminar flame speed of *iso*-octane by destroying the balanced production of $CH_3$ and H because of branching. When the blending ratio of *n*-butanol is increased, the proportion of branching in the fuel blends is decreased, resulting in decreased production of unreactive intermediates and increased laminar flame speed. This has been verified by Dagaut and Togbé.[10] They experimentally investigated the oxidation process of *iso*-octane/*n*-butanol blends in a jet-stirred reactor and found that the mole fraction of unreactive

intermediates of $CH_4$, $C_3H_6$, and $iC_4H_9$ are remarkably decreased with increasing blending ratio of *n*-butanol.

The above kinetic analysis verifies our consideration that the slight increase of laminar flame speed of *iso*-octane/*n*-butanol blends with increasing blending ratio of *n*-butanol is caused by the oxidation kinetics.

**3.3. Markstein Lengths and Diffusional Thermal Stability.** Markstein length is a parameter that quantifies the response of flame propagation to the stretch rate. Additionally, Markstein length represents the diffusional thermal stability of the mixture. A positive Markstein length indicates that the flame is stable, and vice versa. Previous investigations showed that hydrogen and other light hydrocarbon (methane) fuels are more diffusive than the oxidizer (air), and thus increasing the equivalence ratio increases the diffusional thermal stability and Markstein length. In contrast to this, heavy fuels are less diffusive than air, and thus increasing the equivalence ratio reduces the diffusional thermal stability and Markstein length.[30]

Figure 9 gives the Markstein length of *iso*-octane/*n*-butanol–air mixtures as a function of equivalence ratio at three initial temperatures with different blending ratios of *n*-butanol. At all three temperatures, the Markstein length decreases monotonically with increasing equivalence ratio. This is reasonable since both *iso*-octane and *n*-butanol are less diffusive than air, which leads to a decreased Markstein length with increasing equivalence ratio. Additionally, there is a generalized observation in Figure 9 that, at all three temperatures, the absolute value of Markstein length is smallest ($L_b \sim 0$ mm) at a critical equivalence ratio $\phi^*$ ($\phi^* \sim 1.3$). This indicates that, at this equivalence ratio, the effect of flame stretch on flame propagation speed is minimal. Furthermore, there is a generalized crossover $f_{vb}$ dependence of Markstein length. Specifically, at equivalence ratios less than $\phi^*$, Markstein length decreases with increasing blending ratio of *n*-butanol, suggesting that the diffusional thermal stability of the fuel blend–air mixture is decreased with increasimg blending ratio of *n*-butanol, while at equivalence ratios larger than $\phi^*$, Markstein length increases with increasing blending ratio of *n*-butanol, indicating the promoted diffusional thermal stability with increasing blending ratio of *n*-butanol. This observation is consistent with the experimental results in ref 15.

Theoretically, Bechtold and Matalon[30] proposed an explicit expression for the Markstein length as

$$L_b = \delta_l\left[\sigma^{-1}\gamma_1 + \frac{1}{2}Ze(Le-1)\gamma_2\right] \tag{7}$$

where $\gamma_1 = 2\sigma/(\sqrt{\sigma}+1)$, $\gamma_2 = [4/(\sigma-1)][\sqrt{\sigma}-1-\ln(^1/_2)(\sqrt{\sigma}+1)]$, and $Ze$ is the Zeldovich number calculated by

$$Ze = E_a(T_a - T_u)/R^0T_a^2 \tag{8}$$

$E_a$ is overall activation energy; $T_a$ is the flame temperature, which is close to the adiabatic temperature under the assumption of one-step overall reaction with large activation energy; $T_u$ is initial temperature; and $\sigma$ is density ratio, calculated by $\sigma = \rho_u/\rho_b$, where $\rho_u$ is the density of unburned gas and $\rho_b$ is the density of burned gas. $\delta_l$ is laminar flame thickness calculated by[31]

$$\delta_l = \frac{2\lambda}{\rho C_p S_u^0}\left(\frac{T_a}{T_u}\right)^{0.7} \tag{9}$$

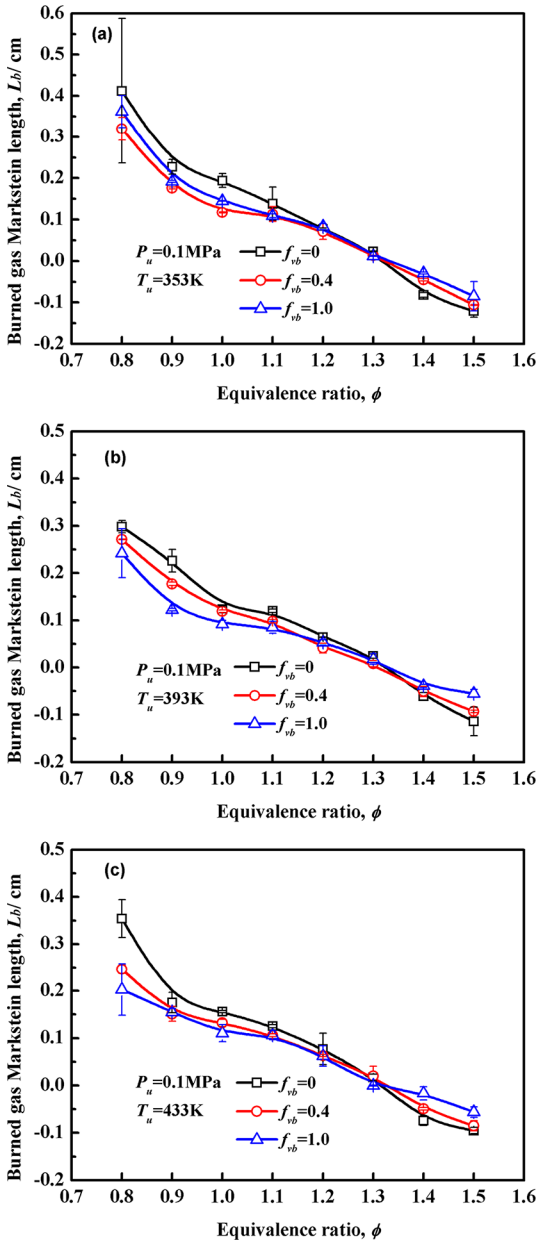


**Figure 9.** Burned gas Markstein length versus equivalence ratios at different blending ratios. (a) $T_u$ = 353 K; (b) $T_u$ = 393 K; (c) $T_u$ = 433 K.

Figure 10 gives the density ratio versus equivalence ratio at different blending ratios. The density ratio varies little with variation of the blending ratio of *n*-butanol; thus, the variation trend of Markstein length with blending ratio of *n*-butanol is determined by laminar flame thickness, Zeldovich number, and Lewis number. The variation trends of laminar flame thickness and Lewis number with the blending ratio of *n*-butanol are demonstrated in Figures 11 and 7, respectively. From the analysis of flame speed in section 3.2, it can be concluded that activation energy and Zeldovich number are decreased with increasing blending ratio of *n*-butanol. At $\phi < \phi^*$, the Lewis number is larger than unity; in this case, with increased blending ratio of *n*-butanol, the term $Ze(Le-1)$ in eq 7 is decreased, resulting in an obvious decrease of Markstein length with increasing blending ratio of *n*-butanol. At $\phi > \phi^*$, the Lewis number is smaller than unity; the term $(Le-1)$ is

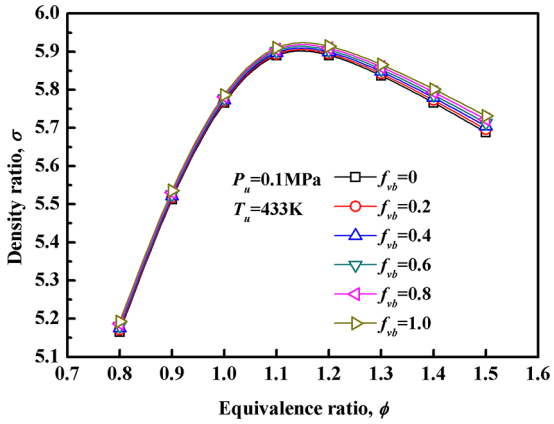


**Figure 10.** Density ratio versus equivalence ratio at different blending ratios.

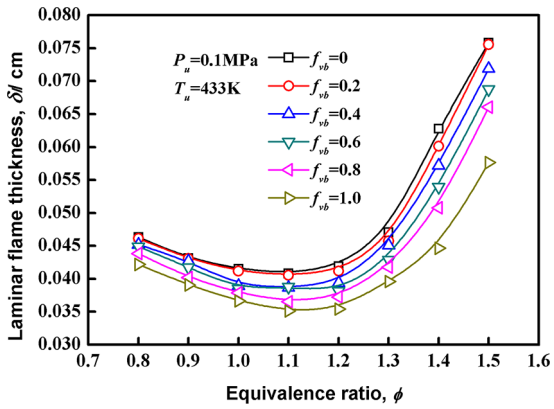


**Figure 11.** Laminar flame thickness versus equivalence ratio at different blending ratios.

negative, and in this case, the decrease of Zeldovich number with increasing blending ratio of *n*-butanol leads to a slight increase in Markstein length.

**3.4. Laminar Flame Speed Correlation.** Laminar flame speeds of fuel–air mixtures versus parameters are useful for practical applications and simulations. A correlation that describes the dependence of laminar flame speed of *iso*-octane/*n*-butanol–air mixtures on equivalence ratio and initial temperature is obtained as[32−35]

$$S_u^0 = S_{u,ref}^0 (T_u/T_u^0)^\alpha \tag{10}$$

where $S_{u,ref}^0$ is the reference laminar flame speed; $T_u^0$ is the reference temperature, which is 353 K in this study; and $\alpha$ is the power exponent, which is a function of equivalence ratio. $\alpha$ and $S_{u,ref}^0$ were fitted on the basis of experimental data by the least-squares method.

For the *iso*-octane–air mixtures,

$$S_{u,ref}^0 = -160.7 + 427.2\phi - 271.6\phi^2 + 44.2\phi^3$$

$$\alpha = 4.15 - 3.28\phi + 1.12\phi^2$$

For the *n*-butanol–air mixtures,

$$S_{u,ref}^0 = -81.1 + 212.9\phi - 73.6\phi^2 - 14.1\phi^3$$

$$\alpha = 5.27 - 5.75\phi + 2.32\phi^2$$

To estimate the laminar flame speeds of the *iso*-octane/*n*-butanol–air mixtures, a good mixing rule is indispensable. Recently, Sileghem et al.[36] proposed a formula by substituting mole fraction with energy fraction in the Le Chatelier's rule-like formula proposed by Di Sarli and Benedetto[37] Considering the similarity of the *iso*-octane/*n*-butanol blends with the gasoline–alcohol blends, we choose the following formula proposed by Sileghem et al.[36] as the mixing rule for the *iso*-octane/*n*-butanol blends in this study:

$$S_{u,blend}^0(\phi) = \frac{1}{\sum_{i-1}^{n} \frac{a_i}{S_{u,i}^0(\phi)}} \tag{11}$$

where $a_i = \Delta H_i^0 x_i / (\sum_{i=1}^{n} H_i^0 x_i)$ is the energy fraction of the *i*th component, $\Delta H_i^0$ is the heat of combustion of the *i*th component, $x_i$ is the mole fraction of the *i*th component, and $S_{u,i}^0$ is the laminar flame speed of the *i*th component.

Generally, the fitted formulas for laminar flame speeds of *iso*-octane/*n*-butanol blend–air mixtures capture the experimental data fairly well, as shown in Figures 4 and 5 The coefficient of determination ($R^2$) is 0.99 and the standard error (SE) is 1.36 cm/s for the correlations.

## 4. CONCLUSIONS

Effects of *n*-butanol addition on laminar flame speeds and Markstein lengths of *iso*-octane/*n*-butanol–air mixtures were studied experimentally over a wide range of equivalence ratios at elevated temperatures.

(1) Laminar flame speed increases with increasing blending ratio of *n*-butanol. This positive dependence of laminar flame speed on blending ratio was interpreted for thermodynamic and diffusive properties. Thermodynamic and diffusive properties exert a negative effect on laminar flame speed with increasing blending ratio of *n*-butanol. The positive dependence of laminar flame speed on blending ratio of *n*-butanol is ascribed to enhanced oxidation kinetics.

(2) There exists a generalized Markstein length behavior. That is, the absolute value of Markstein length reaches its minimum at the critical equivalence ratio ($\phi^* = 1.3$), where the effect of flame stretch on flame propagating speed is the smallest. At equivalence ratios less than the critical equivalence ratio, increasing blending ratio of *n*-butanol decreases the Markstein length, reflecting the fact that addition of *n*-butanol decreases the overall diffusional thermal stability of the binary fuel–air mixtures. At equivalence ratios larger than the critical equivalence ratio, increasing blending ratio of *n*-butanol increases the Markstein length, indicating enhanced diffusional thermal stability.

(3) A correlation of laminar flame speeds as a function of initial temperature, equivalence ratio, and blending ratio of *n*-butanol is given on the basis of experimental data.

## ■ ASSOCIATED CONTENT

### Supporting Information

One table, listing primary data of laminar flame speeds and Markstein lengths for *iso*-octane/*n*-butanol–air mixtures. This material is available free of charge via the Internet at http://pubs.acs.org/.

## AUTHOR INFORMATION


### Corresponding Author

*E-mail chenglongtang@mail.xjtu.edu.cn (C.T.), zhhuang@mail.xjtu.edu.cn (Z.H.); telephone 86-29-82665075; fax 86-29-82668789.


### Notes

The authors declare no competing financial interest.

## ACKNOWLEDGMENTS

This study was supported by the National Natural Science Foundation of China (51136005, 51121092), the Ministry of Education of China (20120201120067), and the National Basic Research Program (2013CB228406).

## NOMENCLATURE

$r_f$ = raw flame radius (cm)
$\rho_u$ = density of unburned gas mixtures (kg/m$^3$)
$\rho_b$ = density of burned gas mixtures (kg/m$^3$)
$S_u^0$ = laminar flame speed (cm/s)
$S_b^0$ = unstretched flame speed of burned gas mixtures (cm/s)
$S_b$ = stretched flame speed of burned gas mixtures (cm/s)
$L_b$ = Markstein length of burned gas mixtures (cm)
$\alpha$ = stretch rate (s$^{-1}$)
$f$ = laminar burning flux (kg/m$^2$·s)
$\lambda$ = thermal conductivity (W/m·K)
$C_p$ = specific heat at constant pressure (J/mol·K)
$Le$ = global Lewis number
$E_a$ = overall activation energy (kJ/mol)
$R_0$ = universal gas constant (J/mol·K)
$T_{ad}$ = adiabatic temperature (K)
$D_m$ = mass diffusivity (m$^2$/s)
$P_u$ = initial pressure (Pa)
$T_u$ = initial temperature (K)
$T_a$ = flame temperature (K)
$\delta_l$ = laminar flame thickness (cm)
$\sigma$ = density ratio
$Ze$ = Zeldovich number
$\phi$ = equivalence ratio
$f_{vb}$ = volume faction of *n*-butanol in *n*-butanol/*iso*-octane blends
$\phi^*$ = critical equivalence ratio

## REFERENCES


(1) Savage, N. Fuel options: the ideal biofuel. *Nature* **2011**, *474* (7352), S9−S11.
(2) Togbé, C.; Halter, F.; Foucher, F.; Mounaim-Rousselle, C.; Dagaut, P. Experimental and detailed kinetic modeling study of 1-pentanol oxidation in a JSR and combustion in a bomb. *Proc. Combust. Inst.* **2011**, *33* (1), 367−374.
(3) Zhao, L.; Ye, L.; Zhang, F.; Zhang, L. Thermal decomposition of 1-pentanol and its isomers: a theoretical study. *J. Phys. Chem. A* **2012**, *116* (37), 9238−9244.
(4) Alasfour, F. N. Butanol—A single-cylinder engine study: availability analysis. *Appl. Therm. Eng.* **1997**, *17* (6), 537−549.
(5) Gu, X.; Huang, Z.; Cai, J.; Gong, J.; Wu, X.; Lee, C.-f. Emission characteristics of a spark-ignition engine fueled with gasoline-n-butanol blends in combination with EGR. *Fuel* **2012**, *93*, 611−617.
(6) Szwaja, S.; Naber, J. D. Combustion of n-butanol in a spark-ignition IC engine. *Fuel* **2010**, *89* (7), 1573−1582.
(7) Dagaut, P.; Togbé, C. Oxidation kinetics of butanol−gasoline surrogate mixtures in a jet-stirred reactor: Experimental and modeling study. *Fuel* **2008**, *87* (15−16), 3313−3321.
(8) Dagaut, P.; Togbé, C. Experimental and modeling study of the kinetics of oxidation of ethanol−gasoline surrogate mixtures (E85 surrogate) in a jet-stirred reactor. *Energy Fuels* **2008**, *22* (5), 3499−3505.
(9) Togbé, C.; Ahmed, A. M.; Dagaut, P. Experimental and modeling study of the kinetics of oxidation of methanol−gasoline surrogate mixtures (M85 surrogate) in a jet-stirred reactor. *Energy Fuels* **2009**, *23* (4), 1936−1941.
(10) Dagaut, P.; Togbé, C. Oxidation kinetics of mixtures of iso-octane with ethanol or butanol in a jet-stirred reactor: Experimental and modeling study. *Combust. Sci. Technol.* **2012**, *184* (7−8), 1025−1038.
(11) Qin, X.; Ju, Y. Measurements of burning velocities of dimethyl ether and air premixed flames at elevated pressures. *Proc. Combust. Inst.* **2005**, *30* (1), 233−240.
(12) Wu, X. S.; Li, Q. Q.; Fu, J.; Tang, C. L.; Huang, Z. H.; Daniel, R.; Tian, G. H.; Xu, H. M. Laminar burning characteristics of 2,5-dimethylfuran and iso-octane blend at elevated temperatures and pressures. *Fuel* **2012**, *95*, 234−240.
(13) Ji, C.; Egolfopoulos, F. N. Flame propagation of mixtures of air with binary liquid fuel mixtures. *Proc. Combust. Inst.* **2011**, *33* (1), 955−961.
(14) Gulder, Ö. L. Laminar burning velocities of methanol, isooctane and isooctane/methanol blends. *Combust. Sci. Technol.* **1983**, *33* (1−4), 179−192.
(15) Broustail, G.; Seers, P.; Halter, F.; Moréac, G.; Mounaim-Rousselle, C. Experimental determination of laminar burning velocity for butanol and ethanol iso-octane blends. *Fuel* **2011**, *90* (1), 1−6.
(16) Broustail, G.; Halter, F.; Seers, P.; Moréac, G.; Mounaïm-Rousselle, C. Experimental determination of laminar burning velocity for butanol/iso-octane and ethanol/iso-octane blends for different initial pressures. *Fuel* **2013**, *106*, 310−317.
(17) Zhang, Z.; Huang, Z.; Wang, X.; Xiang, J.; Wang, X.; Miao, H. Measurements of laminar burning velocities and Markstein lengths for methanol−air−nitrogen mixtures at elevated pressures and temperatures. *Combust. Flame* **2008**, *155* (3), 358−368.
(18) Tang, C.; Zheng, J.; Huang, Z.; Wang, J. Study on nitrogen diluted propane−air premixed flames at elevated pressures and temperatures. *Energy Convers. Manage.* **2010**, *51* (2), 288−295.
(19) Kelley, A.; Law, C. Nonlinear effects in the extraction of laminar flame speeds from expanding spherical flames. *Combust. Flame* **2009**, *156* (9), 1844−1851.
(20) Kelley, A. P.; Liu, W.; Xin, Y. X.; Smallbone, A. J.; Law, C. K. Laminar flame speeds, non-premixed stagnation ignition, and reduced mechanisms in the oxidation of iso-octane. *Proc. Combust. Inst.* **2011**, *33* (1), 501−508.
(21) Liu, W.; Kelley, A. P.; Law, C. K. Non-premixed ignition, laminar flame propagation, and mechanism reduction of n-butanol, iso-butanol, and methyl butanoate. *Proc. Combust. Inst.* **2011**, *33* (1), 995−1002.
(22) Gu, X.; Huang, Z.; Wu, S.; Li, Q. Laminar burning velocities and flame instabilities of butanol isomers−air mixtures. *Combust. Flame* **2010**, *157* (12), 2318−2325.
(23) Bradley, D.; Hicks, R. A.; Lawes, M.; Sheppard, C. G. W.; Woolley, R. The measurement of laminar burning velocities and Markstein numbers for iso-octane−air and iso-octane−n-heptane−air mixtures at elevated temperatures and pressures in an explosion bomb. *Combust. Flame* **1998**, *115* (1−2), 126−144.
(24) Chong, C. T.; Hochgreb, S. Measurements of laminar flame speeds of liquid fuels: Jet-A1, diesel, palm methyl esters and blends using particle imaging velocimetry (PIV). *Proc. Combust. Inst.* **2011**, *33* (1), 979−986.
(25) Davis, S. G.; Law, C. K. Determination of and fuel structure effects on laminar flame speeds of C1 to C8 hydrocarbons. *Combust. Sci. Technol.* **1998**, *140* (1−6), 427−449.
(26) Veloo, P. S.; Wang, Y. L.; Egolfopoulos, F. N.; Westbrook, C. K. A comparative experimental and computational study of methanol, ethanol, and n-butanol flames. *Combust. Flame* **2010**, *157* (10), 1989−2004.
(27) Law, C. K. *Combustion Physics*; Cambridge University Press: Cambridge, U.K., 2006.

(28) Lowry, W. B.; Serinyel, Z.; Krejci, M. C.; Curran, H. J.; Bourque, G.; Petersen, E. L. Effect of methane-dimethyl ether fuel blends on flame stability, laminar flame speed, and Markstein length. *Proc. Combust. Inst.* **2011**, *33* (1), 929−937.
(29) Ji, C.; Sarathy, S. M.; Veloo, P. S.; Westbrook, C. K.; Egolfopoulos, F. N. Effects of fuel branching on the propagation of octane isomers flames. *Combust. Flame* **2012**, *159* (4), 1426−1436.
(30) Bechtold, J. K.; Matalon, M. The dependence of the Markstein length on stoichiometry. *Combust. Flame* **2001**, *127* (1−2), 1906−1913.
(31) Poinsot, T.; Veynante, D. *Theoretical and Numerical Combustion*; R.T. Edwards, Inc: Philadelphia, PA, 2005.
(32) Konnov, A. A. The effect of temperature on the adiabatic laminar burning velocities of $CH_4$−air and $H_2$−air flames. *Fuel* **2010**, *89* (9), 2211−2216.
(33) Konnov, A. A.; Meuwissen, R. J.; de Goey, L. P. H. The temperature dependence of the laminar burning velocity of ethanol flames. *Proc. Combust. Inst.* **2011**, *33* (1), 1011−1019.
(34) Marshall, S. P.; Taylor, S.; Stone, C. R.; Davies, T. J.; Cracknell, R. F. Laminar burning velocity measurements of liquid fuels at elevated pressures and temperatures with combustion residuals. *Combust. Flame* **2011**, *158* (10), 1920−1932.
(35) Liao, S. Y.; Jiang, D. M.; Huang, Z. H.; Shen, W. D.; Yuan, C.; Cheng, Q. Laminar burning velocities for mixtures of methanol and air at elevated temperatures. *Energy Convers. Manage.* **2007**, *48* (3), 857−863.
(36) Sileghem, L.; Vancoillie, J.; Demuynck, J.; Galle, J.; Verhelst, S. Alternative fuels for spark-ignition engines: Mixing rules for the laminar burning velocity of gasoline−alcohol blends. *Energy Fuels* **2012**, *26* (8), 4721−4727.
(37) Di Sarli, V.; Benedetto, A. D. Laminar burning velocity of hydrogen−methane/air premixed flames. *Int. J. Hydrogen Energy* **2007**, *32* (5), 637−646.
(38) Lapuerta, M. N.; García-Contreras, R.; Campos-Fernández, J.; Dorado, M. P. Stability, lubricity, viscosity, and cold-flow properties of alcohol−diesel blends. *Energy Fuels* **2010**, *24* (8), 4497−4502.
(39) Wallner, T.; Miers, S. A.; McConnell, S. A comparison of ethanol and butanol as oxygenates using a direct-injection, spark-ignition engine. *J. Eng. Gas Turbines Power* **2009**, *131* (3), 032802.
(40) Yacoub, Y.; Bata, R.; Gautam, M. The performance and emission characteristics of C 1−C 5 alcohol−gasoline blends with matched oxygen content in a single-cylinder spark ignition engine. *Proc. Inst. Mech. Eng., Part A* **1998**, *212* (5), 363−379.